Detuning dependence of Rabi oscillations in an InAs self-assembled quantum dot ensemble

Takeshi Suzuki, Rohan Singh, Manfred Bayer, Arne Ludwig, Andreas D. Wieck, and Steven T. Cundiff

Phys. Rev. B **97**, 161301 — Published 4 April 2018

DOI: 10.1103/PhysRevB.97.161301

Detuning Dependence of Rabi Oscillations in an InAs Self-Assembled Quantum Dot Ensemble

Takeshi Suzuki,[1,2,*] Rohan Singh,[1,2,†] Manfred Bayer,[3] Arne Ludzwig,[4] Andreas D. Wieck,[4] and Steven T. Cundiff[1,2,‡]

[1] *Physics Department, University of Michigan, Ann Arbor, MI 48109, USA*
[2] *JILA, University of Colorado & National Institute of Standards and Technology, Boulder, Colorado 80309-0440, USA*
[3] *Experimentelle Physik 2, Technische Universtät Dortmund, D-44221 Dortmund, Germany*
[4] *Lehrstuhl fuer Angewandte Festkoerperphysik, Ruhr-Universitaet Bochum, Universitaetsstrasse 150, D-44780 Bochum, Germany*

(Dated: March 6, 2018)

We study the coherent evolution of an InAs self-assembled quantum dot (QD) ensemble in the ultrafast regime. The evolution of the entire frequency distribution is revealed by performing prepulse 2D coherent spectroscopy. Charged and neutral QDs display distinct nonlinear responses arising from 2-level trion and 4-level exciton-biexciton systems, respectively, and each signal is clearly separated in 2D spectra. While the signals for charged QDs are symmetric with respect to the detuning, those for neutral QDs are asymmetric due to the asymmetric 4-level energy structure. Experimental results for charged and neutral QDs are well reproduced by solving the optical Bloch equations, including detuning and excitation-induced dephasing (EID) effects. The temperature dependence suggests that wetting layer carriers play an important role in EID.

PACS numbers: 78.67.Hc, 73.21.La, 78.47.jh

Coherent control is widely used to optically drive a material into a desired state through resonant light-matter interaction. One of the key mechanisms is Rabi oscillation, which enables population inversion in a two-level system; inversion is impossible using incoherent light[1,2]. For resonant excitation, it is possible to attain complete population inversion, *i.e.*, the ground state is entirely depopulated. However, if the light is detuned, the maximum population inversion decreases[3,4]. Although a highly inverted population, which can only be achieved through Rabi oscillations using on-resonance excitation, is favorable for many applications including lasers, detuning the light from the transition frequency results in new phenomena. Examples include larger population inversion by using phonon assistance[5–7] or inversion by chirped pulses via rapid adiabatic passage[8]. Depending on the desired outcome, one can design the control field when a system of interest is a homogeneous ensemble or a single object.

For an inhomogeneously broadened ensemble displaying large fluctuation in transition frequencies, however, the resonant and off-resonant frequency groups simultaneously experience the same control field. This effect is especially evident when the system is driven by a spectrally broad femtosecond laser (∼100 fs). While coherent control of ensemble systems is desired because a large number of oscillators provide a statistical advantage in potential applications[9–11] as well as promising playground to explore collective effects[12,13], detuning effects must be circumvented to prevent smearing out the coherent signals. In semiconductor quantum dots (QDs), many optical techniques have been employed to overcome inhomogeneous broadening[14–17]. Recently, two-dimensional coherent spectroscopy (2DCS) has been used to disentangle homogeneous and inhomogeneous broadening in semiconductor nanostructures including QDs[18–21]. 2DCS has also been used to track populations in a resonant frequency group in a QD ensemble after coherent excitation[22].

Here, we demonstrate coherent control over the entire frequency distribution for both neutral and charged QDs. The behavior of the trions' 2-level system appears symmetric with respect to the center energy of excitation laser. However, the exciton-biexciton 4-level system exhibits an asymmetric behavior. Although such a behavior is counter-intuitive, it reflects the asymmetric 4-level energy structure of the exciton-biexciton system. The experimental data is well reproduced by calculating 2-level and 4-level optical Bloch equations (OBEs) including detuning and excitation-induced dephasing (EID). We suggest one of the dominant EID sources is wetting layer carriers through temperature dependent measurements.

Figure 1 (a) shows a schematic of the experiment. In addition to conventional 2DCS, a prepulse coherently prepares populations in the ground, trion, exciton, and biexciton states. Three 2DCS pulses are incident on the sample in the rephasing (photon-echo) time-ordering. The delays between pulses A*, B, C, and the emitted FWM signal are denoted as τ, T, and t, respectively. The delay between the prepulse and the 2DCS pulse A* is denoted as Δt. In this work we set $\Delta t = 15$ ps, which is more than one order of magnitude shorter than the population decay times in each state[22]. The prepulse and each pulse used in 2DCS have the same spectral profile and are generated by a mode-locked Ti:sapphire laser at a repetition rate of 76 MHz. The pulses have a bandwidth of 14.8 meV (full width at half maximum) as shown in the inset of Fig. 2(a). The spatial profile of the prepulse is twice as broad as the 2D pulses in order to reduce spatial inhomogeneity in excitation.

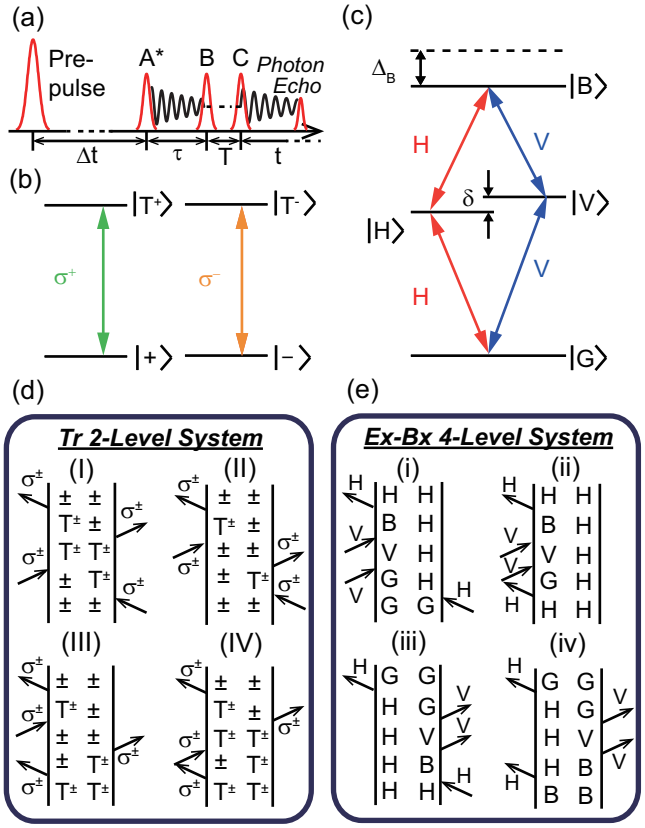

FIG. 1. (a) Schematic of the prepulse 2DCS experiment. Delays between prepulse, A*, B, C, and signal are denoted as Δt, τ, T, t, respectively. (b) The energy level diagram representing the trion transition ($|+\rangle$ ($|-\rangle$) $\leftrightarrow$ $|T^+\rangle$ ($|T^-\rangle$)) by right(left) circularly polarized light ($\sigma^+(\sigma^-)$). (c) The energy level diagram representing the transitions between the ground ($|$G$\rangle$), horizontal ($|$H$\rangle$) and vertical ($|$V$\rangle$) excitons, and biexciton ($|$B$\rangle$) states by horizontally (H) and vertically (V) polarized light. δ is the fine structure splitting energy between $|$H$\rangle$ and $|$V$\rangle$, and Δ_B is the biexciton binding energy. The quantum paths for trion 2-level system (d) and exciton-biexciton 4-level system (e).

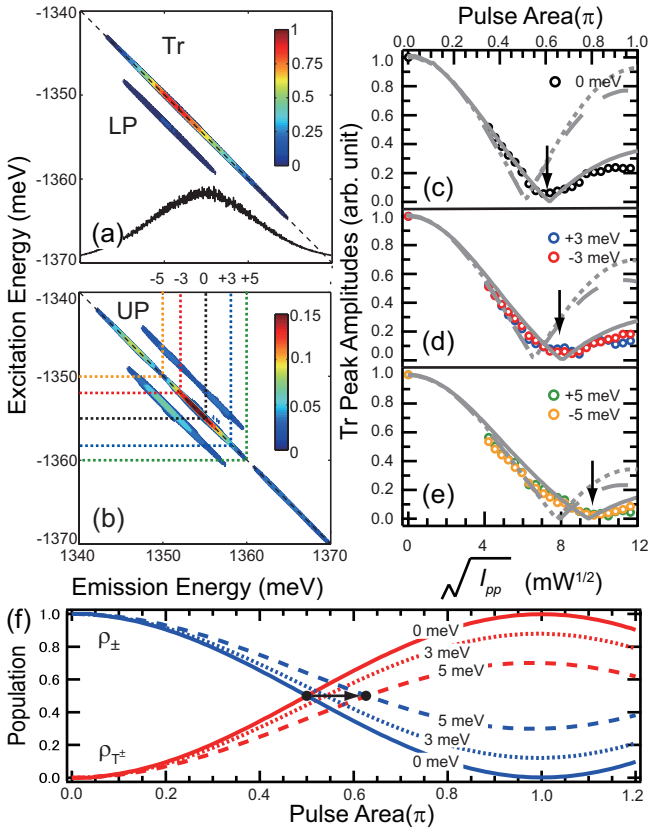

FIG. 2. 2D rephasing amplitude spectra using prepulse powers of (a) 0 and (b) 94 mW. (c)-(e) Peak amplitudes of 2D rephasing spectra for the Tr peak belonging to resonant frequency group ($\Delta = 0$ meV) and detuned frequency groups ($\Delta = \pm3, \pm5$ meV). The dashed and solid gray lines are simulation results for $|\rho_\pm - \rho_{T\pm}|$ with γ^* of 0 and 2 meV, respectively. The dotted lines are the result with $\gamma^* = 0$ meV without spatial averaging. The bottom axes are for the experimental data, whereas the top axes are for simulation results. (f) Simulation results of $\rho_\pm$ and $\rho_{T\pm}$ with different detunings denoted at each line without considering any damping. The arrow shows that the pulse area necessary to achieve $\rho_\pm = \rho_{T\pm}$ increases with Δ.

The sample comprises 10 layers of InAs/GaAs self-assembled QDs, which was used in previous studies[22,23]. The prepulse was focused to a diameter of 135 μm and QD density is $\sim 10^{10}$/cm^2 per layer, which results in an excitation of $\sim 10^7$ QDs in the ensemble. The sample was unavoidably doped during growth, resulting in approximately half of the QDs being charged with a hole, which forms a trion with a photo excited electron and hole pair[23].

The energy structure and selection rules for InAs QDs change significantly depending on the existence of a hole in a QD. Figure 1(b) shows the energy level diagram of the trion system. From a hole in the spin up(down) state, $|+\rangle$ ($|-\rangle$), a spin up(down) trion state, $|T^+\rangle$ ($|T^-\rangle$), is created by right(left) circularly polarized light, $\sigma_+(\sigma_-)$. Since spin up and down states are degenerate without external field, a charged QD offers a doubly degenerate 2-level system. Neutral excitons are described by the 4-level system shown in Fig. 1(c). The two non-degenerate horizontal ($|H\rangle$) and vertical ($|V\rangle$) exciton states have orthogonal linearly polarized transitions from the ground state $|G\rangle$ due to the cylindrical-symmetry breaking. The energy of the biexciton state $|B\rangle$ is lower than the sum of the two exciton energies by the biexciton binding energy ($\Delta_B = 3.3\pm0.03$ meV)[24,25], which is much larger than the fine structure splitting energy ($\delta = 19\pm1$ μeV) between $|H\rangle$ and $|V\rangle$[26,27,31]. Both Δ_B and δ depend on QD size, so they will vary across the ensemble, however the change is small so we ignore it for the analysis presented here. The sample is aligned such that the eigenstates are along the horizontal (H) and vertical (V) directions. The temperature is 10 K unless mentioned otherwise.

To observe the signals attributed to neutral and

charged QDs separately in 2D spectra, we use a cross-linearly polarized excitation and detection scheme, i.e. $HVVH$ for A*, B, C and the signal[24]. Figure 2(a) shows a 2D rephasing amplitude spectrum without the prepulse. The spectrum features two peaks that are inhomogeneously broadened along the diagonal direction, indicated by the dashed black line, due to QD size dispersion. The peak labeled Tr arises from the trion nonlinear response, whereas the peak labeled LP, arising from the biexciton, is red-shifted from the diagonal along the emission energy axis by the biexciton binding energy. The polarization for the prepulse is H, which is expressed in the circular basis as $1/\sqrt{2}\,(\sigma_+ + \sigma_-)$. The pre-pulse transfers the population from $|\pm\rangle$ to $|T^{\pm}\rangle$ for the trion system, whereas it transfers the population from $|G\rangle$ to $|H\rangle$ and $|H\rangle$ to $|B\rangle$ for the exciton-biexciton system. When the pre-pulse is incident on the sample, a new peak labeled as upper peak (UP) in Fig. 2(b) appears due to population transfer to $|H\rangle$ and $|B\rangle$. Because the center energy of the prepulse spectrum is 1355 meV, the signals for the resonant frequency group can be tracked at the position where the black dotted line labeled as 0 intersects each peak, as shown in Fig. 2(b). Similarly, the detuning effect can be elucidated by focusing on different positions in each peak. In Fig. 2(b), amplitudes of each peak at intersections with the blue/red dotted line labeled as 3/-3 correspond to signals belonging to $\Delta = +/-3$ meV. Further detuning effects of $\Delta = +/-5$ meV can be observed along the green/orange dotted line, where Δ is the detuning.

We first discuss the response of the 2-level system of trions (Figs. 1(b) and 1(d)). From the relationship between linear and circular polarizations, $HVVH$ includes $\sigma_+\sigma_+\sigma_+\sigma_+$ and $\sigma_-\sigma_-\sigma_-\sigma_-$ as combinations relevant to quantum pathways for trions. The trion peak (Tr) in Fig. 2(a) corresponds to the quantum pathways starting from the ground state shown in Fig. 1(d)-(I) and 1(d)-(II). With the prepulse, other quantum pathways, starting with population in the trion state (Figs.1(d)-(III) and 1(d)-(IV)) also contribute to the 2D signal at the position of the Tr in the 2D spectrum with the opposite sign compared to the signal from Figs. 1(d)-(I) and 1(d)-(II). As a result, the Tr represents the difference between the ground state population $\rho_{\pm}$ and the trion state population $\rho_{T^{\pm}}$. As is clearly seen in Fig. 2(b), Tr significantly decreases after the arrival of the pre-pulse.

Figures 2(c)-2(e) show peak amplitudes for the Tr belonging to the resonant frequency group ($\Delta = 0$ meV) and detuned frequency groups ($\Delta = \pm 3, \pm 5$ meV). They are plotted as a function of square root of prepulse power $\sqrt{I_{pp}}$, which is proportional to the pulse area explicitly defined later. The detuning dependence is symmetric with respect to absolute value of detuning for both red- and blue-detuned components. Additionally, as $|\Delta|$ increases, the $\sqrt{I_{pp}}$ for the minimum increases, clearly shown by the black arrows. This trend is understood by considering 2-level system with varying detuning. Figure 2 (f) shows the simulation result of $\rho_{\pm}$ and $\rho_{T^{\pm}}$ with different detunings without considering any damping. The required power for zero crossing increases for increasing $|\Delta|$ shown by a black arrow, successfully reproducing the observed trend.

For quantitative insight, we perform the calculation using the optical Bloch equations (OBEs) for the 2-level system

$$\dot{\rho}_{T^{\pm}} = -i\Omega_{\pm}(t)\,(\rho_{10} - \rho_{01}) - \Gamma_{T^{\pm}}\rho_{T^{\pm}} \quad (1)$$

$$\dot{\rho}_{01} = -i\Omega_{\pm}(t)\,(1 - 2\rho_{T^{\pm}}) - (\gamma_{01} + \kappa(t) - i\Delta)\,\rho_{01}, \quad (2)$$

where $\Omega_{\pm}(t)$ is Rabi frequency, ρ_{01} is the trion coherence in the rotating frame, $\Gamma_{T^{\pm}}$ and γ_{01} are the population and coherence decay rate of trions, respectively, and $\kappa(t)$ is time-dependent additional dephasing rate due to EID. Averaging of the Rabi frequency due the spatial variation of the pre-pulse power is taken into account. The details and parameters used in the calculation are found in Ref.[28]. Dotted lines in Figs. 2(c)-2(e) show the simulation results for the population differences $|\rho_{\pm} - \rho_{T^{\pm}}|$ without additional dephasing ($\kappa(t) = 0$) and spatial averaging. Reduction in the effective pulse area due to spatial averaging is considered in dashed line. Although they have a good qualitative agreement, the experimental data deviates from simulation at higher power. This phenomenon is caused by EID, and has been intensively examined through the phonon and wetting layer models[32–38]. Because the wetting layer model is relevant in our experiments as discussed later, we use, $\kappa(t) = \gamma^* p(t)$, as the form of the EID where γ^* is the EID rate and $p(t)$ is the wetting carrier occupation given by the square of pulse area, $\Theta(t) = \int_{-\infty}^{t} \Omega_{\pm}(t')dt'$. Solid lines in Figs. 2(c)-2(e) show the results of calculations with $\gamma^* = 2$ meV, plotted as a function of pulse area. The experimental data and calculation have excellent agreement.

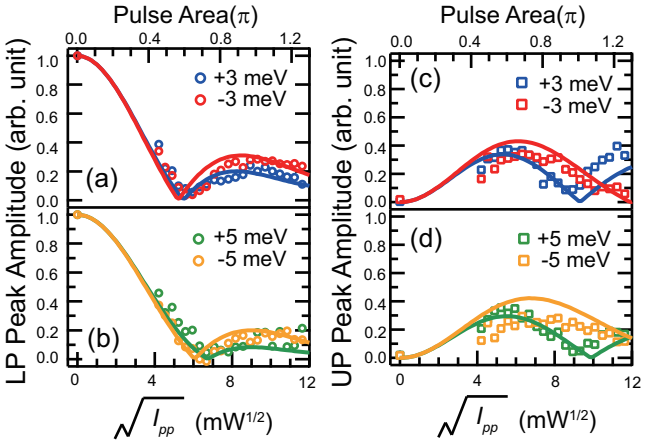

FIG. 3. Peak amplitudes of 2D rephasing spectra for the LP ((a) and (b)) and UP ((c) and (d)) belonging to detuned frequency groups ($\Delta = \pm 3, \pm 5$ meV). Solid lines are simulation results for $|\rho_G - \rho_H|$ in (a) and (b) and $|\rho_H - \rho_B|$ in (c) and (d). The bottom axes are for the experimental data, whereas the top axes are for simulation results.

Next, we discuss the exciton-biexciton 4-level system (Figs. 1(c) and 1(e)). Since the results for the resonant frequency group ($\Delta = 0$ meV) were previously studied in detail[22], we focus here on the detuned frequency groups. Figures 3 (a) and 3(c) show peak amplitudes for the LP and UP for $\Delta = \pm 3$ meV, respectively. The behavior for $\Delta = +3$ meV clearly differs from that for $\Delta =$ - 3 meV. While the UP for $\Delta = +3$ meV has a minimum around $\sqrt{I_{PP}} = 8.5$ mW$^{-1/2}$, the UP for $\Delta =$ -3 meV needs $\sqrt{I_{PP}} = 12$ mW$^{-1/2}$ before a minimum occurs. This difference is apparently counter-intuitive from Eq. (1) and different from the trions' behavior. This *asymmetric* behavior with respect to the sign of detuning results from the exciton-biexciton 4-level system (Figs. 1(c)). For the exciton-biexciton system, the resonant frequency group ($\Delta = 0$ meV) corresponds to QDs whose energy separation between $|G\rangle$ and $|H\rangle$ is the same as the center energy of the prepulse (1355 meV). The biexciton binding energy Δ_B lowers the transition energy between $|H\rangle$ and $|B\rangle$ by 3.3 meV compared to the $|G\rangle$ to $|H\rangle$ transition. Consequently, frequency groups of $\Delta = +3$ and -3 meV no longer have a symmetric relationship with respect to $|H\rangle$ to $|B\rangle$ transition, although they remain symmetric with respect to $|G\rangle$ to $|H\rangle$ transition. This asymmetric relationship is confirmed for the higher detuned frequency groups of $\Delta = +5$ and -5 meV shown in Figs. 3(b) and 3 (d).

To confirm these results, we performed calculations using the OBEs for 4-level system including EID with $\gamma^* = 0.5$ meV. Each parameter is chosen to reproduce experimental data most satisfactorily. The details are found in Ref.[28]. The solid lines in Figs. 3 show the calculation results. The population differences $|\rho_G - \rho_H|$ for $\Delta = \pm 3$ meV and ± 5 meV are shown in Figs. 3(a) and 3(c), respectively, whereas $|\rho_H - \rho_B|$ are shown in Figs. 3(b) and 3(d). The simulations successfully capture the observed asymmetric behavior. The EID for excitons and biexcitons (0.5 meV) is less than for trions (2 meV), which may suggest that the charged QDs interacts with wetting layer carriers more strongly through enhanced Coulomb interactions.

Finally, we consider EID mechanisms relevant to our experimental conditions. Among EID mechanisms, the LA phonon mediated model is frequently used to explain the damping of Rabi oscillation in semiconductor QDs[33–37] because the damping effects become relevant at high power. Instead, we employ the wetting layer model, in which carriers created in the wetting layers by the laser pulses contribute to the additional dephasing, schematically shown in Fig. 4(a). Due to the coupling between bound exciton states in QDs and continuous states in wetting layers, the existence of crossed transition involving bound electron (hole) states and continuous hole (electron) states have been confirmed as a broad background[39,40]. Wetting layer carriers can be excited non-resonantly, and are especially evident in the situation where the higher states are pumped to observe the Rabi oscillation because such a pump has higher energy than ground state transition and is more likely to excite crossed transition[32,38]. Although we resonantly excite the transition between ground bound states both in trion and exciton-biexciton systems, the laser is spectrally broader (14.8 meV) and can cover crossed transitions. In addition, the transition energy between the lowest bound hole and electron states for a strongly confined QD (the left QD in Fig. 4(a)) corresponds to the cross transition energy for a loosely confined QD (the right QD in Fig. 4(a)) because of the inhomogeneity of around 20 meV in FWHM in our QD ensemble. Thus, our situation is more likely to create wetting layer carriers than typical studies with spectrally narrow (0.1-1 meV) laser targeting a single QD.

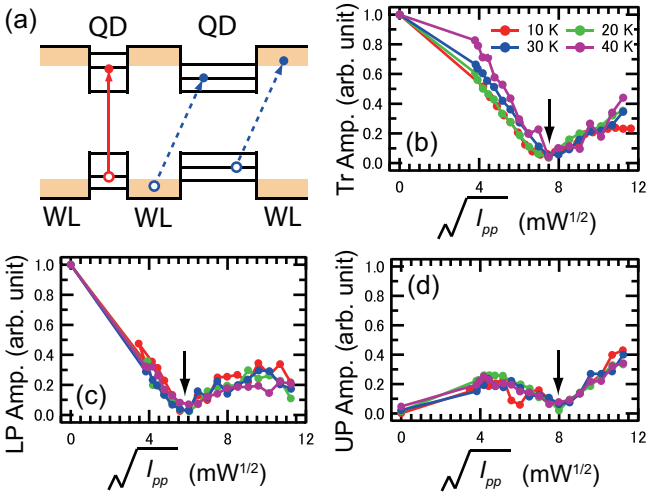

FIG. 4. (a) Schematics of wetting layer model. The red solid arrow represents the transitions between bound states in a QDs whereas blue dashed lines represent crossed transitions. (b) - (d) Temperature-dependent Tr, LP, and UP amplitude belonging to the resonant frequency group. Black arrows show zero crossing points.

To validate this assumption, we performed temperature-dependent measurements because the parameters for Rabi oscillation are reported to significantly depend on the lattice temperature in the LA phonon mediated model. Figure 4(b)-4(d) show Tr, LP, and UP amplitude belonging to the resonant frequency group with varying lattice temperature from 10 to 40 K. As are shown in black arrows, the minimum points of peaks with respect to the pump power do not change with temperature. This invariance is clearly different from reports explaining temperature-dependent behaviors in phonon mediated model, where the pump power necessary to achieve 2π pulse changes significantly depending on lattice temperature [36]. Furthermore, the symmetry of the trions' signal suggests the minimal role played by LA phonons, which would give assymetric signature [41]. Although the observed EID is explained by the wetting layered model in this work, other mechanisms should be considered. Since the Rabi energy at the pulse area of π in this work is around 70 meV

(17 THz), much higher than LA phonons (a few meV), higher energy transitions such as LO phonons (32 meV) [42] or excited states may play a role.

In conclusion, we have investigated the generalized Rabi oscillation both for the 2-level trion system and excitons-biexcitons 4-level system in an InAs self-assembled QD ensemble by using the prepulse 2DCS technique. Experimental data are well reproduced by solving 2-level and 4-level OBEs including detuning and EID effects. The origin of EID is explained by the wetting layer model. We successfully demonstrate that 2DCS can unveil coherent evolutions in the entire frequency group of neutral and charged QDs.

The work at JILA & University of Michigan was primarily supported by the Chemical Sciences, Geosciences, and Energy Biosciences Division, Office of Basic Energy Science, Office of Science, U.S. Department of Energy under Awards No. DE-FG02-02ER15346 and DE-SC0015782. T. S. acknowledges support by Japan Society for the Promotion of Science (JSPS). A.D.W. gratefully acknowledges support of DFG-TRR160Z1, BMBF - Q.com-H 16KIS0109, and the DFH/UFA CDFA-05-06.

* Current address: Institute for Solid State Physics, University of Tokyo, Kashiwa, Chiba 277-8581, Japan
† Current address: Chemistry Division, Los Alamos National Laboratory, Los Alamos, NM 87545, USA
‡ cundiff@umich.edu

[1] T. H. Stievater, Xiaoqin Li, D. G. Steel, D. Gammon, D. S. Katzer, D. Park, C. Piermarocchi, and L. J. Sham, Phys. Rev. Lett. **87**, 133603 (2001).
[2] H. M. Gibbs, Phys. Rev. A **8**, 446 (1973).
[3] N. Rosen and C. Zener, Phys. Rev. **40**, 502-507 (1932)
[4] L. Allen and J. H. Eberly, *Optical Resonance and Two-Level Atoms* (Dover Publications Inc., New York, 1987).
[5] M. Glässl, A. M. Barth, and V. M. Axt, Phys. Rev. Lett. **110**, 147401 (2013).
[6] J. H. Quilter, A. J. Brash, F. Liu, M. Glässl, A. M. Barth, V. M. Axt, A. J. Ramsay, M. S. Skolnick, and A. M. Fox, Phys. Rev. Lett. **114**, 137401 (2015).
[7] S. Bounouar, M. Müller, A. M. Barth, M. Glässl, V. M. Axt, and P. Michler, Phys. Rev. B **91**, 161302 (R) (2015).
[8] T. Kaldewey, S. Lüker, A. V. Kuhlmann, S. R. Valentin, J. -M. Chauveau, A. Ludwig, A. D. Wieck, D. E. Reiter, T. Kuhn, and R. J. Warburton, Phys. Rev. B **95**, 241306(R) (2017).
[9] Y. Arakawa and H. Sakaki, Appl. Phys. Lett. **40**, 939 (1982).
[10] M. Korarczik, N. Owschimikow, J. Korn, B. Lingnau, Y. Kaptan, D. Bimberg, E. Schöll, K. Lüdge, and U. Woggon, Nat. Commun. **4**, 2953 (2013).
[11] J. J. Finley, M. Skalitz, M. Arzberger, A. Zrenner, G. Böhm, and G. Abstreiter, Appl. Phys. Lett. **73**, 2618 (1998).
[12] M. Scheibner, Thomas Schmidt, L. Worschech, A. Forchel, G. Bacher, T. Passow, and D. Hommel, Nat. Phys. **3**, 106 (2007).
[13] Y. O. Dudin, L. Li, F. Bariani, and A. Kuzmich, Nat. Phys. **105**, 140502 (2012).
[14] J. J. Berry, M. J. Stevens, R. P. Mirin, and K. I. Silverman, Appl. Phys. Lett. **88**, 061114 (2006).
[15] L. Yang, P. Glasenapp, A. Greilich, D. Reuter, A. D. Wieck, D. R. Yakovlev, M. Bayer, and S. A. Crooker, Nat. Commun. **5**, 4949 (2014).
[16] P. Borri, W. Langbein, S. Schneider, U. Woggon, R. L. Sellin, D. Ouyang, and D. Bimberg, Phys. Rev. Lett. **87**, 157401 (2001).
[17] S. V. Poltavtsev, M. Salewski, Y. V. Kapitonov, I. A. Yugova, I. A. Akimov, C. Schneider, M. Kamp, S. Höfling, D. R. Yakovlev, A. V. Kavokin, and M. Bayer, Phys. Rev. B **93**, 121304 (R) (2016).
[18] A. D. Bristow, D. Karaiskaj, X. Dai, T. Zhang, C. Carlsson, K. R. Hagen, R. Jimnez, and S. T. Cundiff, Rev. Sci. Instrum. **80**, 073108f (2009).
[19] M. E. Siemens, G. Moody, H. Li, A. D. Bristow, and S. T. Cundiff, Opt. Express **18**, 17699 (2010).
[20] G. Moody, M. E. Siemens, A. D. Bristow, X. Dai, D. Karaiskaj, A. S. Bracker, D. Gammon, and S. T. Cundiff, Phys. Rev. B **83**, 115324 (2011).
[21] J. Kasprzak, S. Portolan, A. Rastelli, L. Wang, J. D. Plumhof, O. G. Schmidt, and W. Langbein, New J. Phys. **15**, 055006 (2013).
[22] T. Suzuki, R. Singh, M. Bayer, A. Ludwig, A. D. Wieck, and S. T. Cundiff, Phys. Rev. Lett. **117**, 157402 (2016).
[23] G. Moody, R. Singh, H. Li, I. A. Akimov, M. Bayer, D. Reuter, A. D. Wieck, and S. T. Cundiff, Phys. Rev. B **87**, 045313 (2013).
[24] G. Moody, R. Singh, H. Li, I. A. Akimov, M. Bayer, D. Reuter, A. D. Wieck, A. S. Bracker, D. Gammon, and S. T. Cundiff, Phys. Rev. B **87**, 041304(R) (2013).
[25] S. Rodt, A. Schliwa, R. Heitz, V. Türck, O. Stier, R. L. Sellin, M. Strassburg, U. W. Pohl, and D. Bimberg, Phys. Stat. Solidi B **234**, 354 (2002).
[26] M. Bayer, G. Ortner, O. Stern, A. Kuther, A. A. Gorbunov, A. Forchel, P. Hawrylak, S. Fafard, K. Hinzer, T. L. Reinecke, S. N. Walck, J. P. Reithmaier, F. Klopf, and F. Schäfer, Phys. Rev. B **65**, 195315 (2002).
[27] G. Moody, R. Singh, H. Li, I. A. Akimov, M. Bayer, D. Reuter, A. D. Wieck, and S. T. Cundiff, Solid State Commun. **163**, 65 (2013).
[28] See Supplemental Material at ... for details of the calculations, which includes Refs. [28-31].
[29] Shaul Mukamel, *Principles of Nonlinear Optical Spectroscopy*, (Oxford University Press, New York, 1995).
[30] Robert W. Boyd, *Nonlinear Optics*, (Academic Press, Orlando, 2008).
[31] W. Langbein, P. Borri, U. Woggon, V. Stavarache, D. Reuter, and A. D. Wieck, Phys. Rev. B **70**, 033301 (2004).
[32] Q. Q. Wang, A. Muller, P. Bianucci, E. Rossi, Q. K. Xue, T. Takagahara, C. Piermarocchi, A. H. MacDonald, and C. K. Shih, Phys. Rev. B **72**, 035306 (2005).
[33] J. Förstner, C. Weber, J. Danckwerts, and A. Knorr, Phys. Rev. Lett. **91**, 127401 (2003).
[34] A. Vagov, M. D. Croitoru, V. M. Axt, T. Kuhn, and F. M. Peeters, Phys. Rev. Lett. **98**, 227403 (2007).
[35] A. J. Ramsay, Achanta Venu Gopal, E. M. Gauger, A. Nazir, B. W. Lovett, A. M. Fox, and M. S. Skolnick, Phys. Rev. Lett. **104**, 017402 (2010).
[36] A. J. Ramsay, T. M. Godden, S. J. Boyle, E. M. Gauger,

A. Nazir, B. W. Lovett, A. M. Fox, and M. S. Skolnick, Phys. Rev. Lett. **105**, 177402 (2010).
[37] Léonard Monniello, Catherine Tonin, Richard Hostein, Aristide Lemaitre, Anthony Martinez, Valia Voliotis, and Roger Grousson, Phys. Rev. Lett. **111**, 026403 (2013).
[38] J. M. Villas-Bôas, Sergio E. Ulloa, and A. O. Govorov, Phys. Rev. Lett. **94**, 057404 (2005).
[39] Y. Toda, O. Moriwaki, M. Nishioka, and Y. Arakawa, Phys. Rev. Lett. **82**, 4114 (1999).
[40] A. Vasanelli, R. Ferreira, and G. Bastard, Phys. Rev. Lett. **89**, 216804 (2002).
[41] A. J. Ramsay, T. M. Godden, S. J. Boyle, E. M. Gauger, A. Nazir, B. W. Lovett, Achanta Venu Gopal, A. M. Fox, and M. S. Skolnick, J. Appl. Phys. **109**, 102415 (2011).
[42] R. Heitz, M. Grundmann, N. N. Ledentsov, L. Eckey, M. Veit, D. Bimberg, V. M. Ustinov, A. Yu. Egorov, A. E. Zhukov, P. S. Kop'ev, and Zh. I. Alferov, Appl. Phys. Lett. **68**, 361 (1996).